SYNTHESIS AND COMPUTATIONAL STUDIES OF MOLECULAR STRUCTURE AND VIBRATIONAL SPECTRA OF 2-AMINO-4-(4-NITROPHENYL)-4*H*-PYRANO-[3,2-*h*]QUINOLINES[**]

P. Kour, A. Kumar, A. Uppal, Y. Khajuria, V. K. Singh[*]

Shri Mata Vaishno Devi University, Faculty of Sciences, India; e-mail: vivekksingh2005@gmail.com

We have disclosed the synthesis of pyranoquinoline derivatives via a one-pot reaction of 4-nitrobenzaldehyde, malononitrile/ethyl cyanoacetate and 8-hydroxyquinoline using 30 mol.% DMAP in ethanol under reflux conditions. The Fourier transform infrared spectra of ethyl 2-amino-4-(4-nitrophenyl)-4H-pyrano[3,2-h]quinoline-3-carboxylate were recorded within the range 4000–400 cm^{-1}. The Hartree–Fock and density functional theory on the 6-311G basis set have been utilized to calculate molecular geometry, vibrational frequencies, atomic charges and thermodynamic parameters. Further, the vibrational energy distribution analysis program was applied to assign the vibrational wavenumbers based on potential energy distribution. The HOMO–LUMO energies, the temperature dependence of the thermodynamic properties and the total electron density, and molecular electrostatic potential maps are also studied.

Keywords: *Hartree–Fock, density functional theory, Fourier transform infrared spectra, vibrational energy distribution analysis, HOMO–LUMO.*

СИНТЕЗ И РАСЧЕТ МОЛЕКУЛЯРНОЙ СТРУКТУРЫ И КОЛЕБАТЕЛЬНЫХ СПЕКТРОВ 2-АМИНО-4-(4-НИТРОФЕНИЛ)-4*H*-ПИРАНО-[3,2-*h*] ХИНОЛИНОВ

P. Kour, A. Kumar, A. Uppal, Y. Khajuria, V. K. Singh[*]

УДК 539.194

Университет Шри Мата Вайшно Деви, Индия; e-mail: vivekksingh2005@gmail.com

(Поступила 17 мая 2018)

Предложен способ синтеза производных пиранохинолина посредством реакции в одном сосуде 4-нитробензальдегида, малононитрил/этилцианоацетата и 8-гидроксихинолина с использованием 30 мол.% DMAP в этаноле в условиях противопотока. Для этил-2-амино-4-(4-нитрофенил)-4H-пирано[3,2-h]хинолин-3-карбоксилата получены ИК спектры с преобразованием Фурье в диапазоне 4000–400 см$^{-1}$. С помощью приближения Хартри–Фока и теории функционала плотности на основе базисного набора 6-311G проведен расчет геометрии молекул, частот колебаний, атомных зарядов и термодинамических параметров. Для определения колебательных волновых чисел применена программа анализа распределения колебательной энергии на основе распределения потенциальной энергии. Изучены энергии HOMO–LUMO, температурная зависимость термодинамических свойств и полной электронной плотности, распределение молекулярного электростатического потенциала.

Ключевые слова: *приближение Хартри–Фока, функциональная теория плотности, инфракрасные спектры с преобразованием Фурье, анализ распределения колебательной энергии, HOMO–LUMO.*

[**]Full text is published in JAS V. 86, No. 4 (http://springer.com/10812) and in electronic version of ZhPS V. 86, No. 4 (http://www.elibrary.ru/title_about.asp?id=7318; sales@elibrary.ru).

Introduction. Pyran and its derivatives represent an essential structural unit and are commonly found in several natural products [1]. They also possess a broad spectrum of biological activities like antimicrobial [2, 3], antitumor [4], antitubercular [5], antioxidant [6], antiviral [7, 8], antiproliferative [9, 10], and diuretic [11]. Further, these molecules are known to be extensively used as photoactive materials [12], and light emitting diodes [13].

Quinolines, another class of heterocyclic compounds, have received great attention due to their broad range of biological properties such as antimalarial [14], antifungal [15], antibacterial [16, 17], anti-inflammatory [18], and antiviral [19]. Additionally, quinolines have also been utilized as sensors [20] and OLEDs [21]. Taking into account the significance of pyran and quinoline derivatives, many reports are available in the literature on the synthesis and characterization of these condensed pyranoquinolines. However, these methods suffer from one or more disadvantages, and therefore it is still beneficial to develop a new protocol to synthesize hybrid complex molecules containing both these moieties.

Domino reactions have played a crucial role in the construction of diverse heterocycles possessing potential biological applications. Domino synthesis provides an eco-friendly pathway for diversity-oriented synthesis with the advantage of a minimum number of steps, thus minimizing wastage and allowing high productivity [22, 23].

Further, after careful survey of the literature, we have not found any theoretical studies being carried out for ethyl 2-amino-4-(4-nitrophenyl)-4*H*-pyrano[3,2-*h*]quinoline-3-carboxylate ($C_{21}H_{17}N_3O_5$), an important heterocyclic molecule of biological significance . In view of the abovementioned reasons and our interest in the synthesis of heterocyclic compounds of biological significance, we have developed a new method for the preparation of pyranoquinoline derivatives *via* the tandem Knoevenagel–Michael reaction as outlined in scheme 1 and also attempted to provide a complete insight into various theoretical molecular parameters using the Gaussian 09 program [24].

At the outset, the reaction mixture consisting of 1 mmol each of 4-nitrobenzaldehyde, malononitrile/ethyl cyanoacetate, 8-hydroxyquinoline and a catalytic amount of DMAP (30 mol.%) was heated under reflux in 5 mL of EtOH (Scheme 1). After the appropriate time, the crude products were purified by column chromatography to provide the desired product, which was further confirmed by ^{1}H NMR and IR spectral studies.

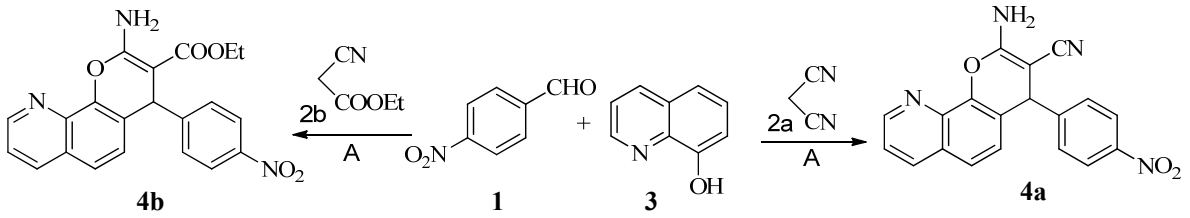

A = DMAP (30 mol.%), EtOH, reflux

Scheme 1. Synthesis of pyranoquinoline derivatives.

Next, we used the Gaussian 09 program [24] to calculate optimized geometry, atomic charges, vibrational frequencies, thermodynamic properties, and molecular parameters by applying the Hartree–Fock (HF) and density functional theory (DFT) on the 6-311G basis set. We then studied the complete molecular structure including the vibrational characteristics of ethyl 2-amino-4-(4-nitrophenyl)-4*H*-pyrano[3,2-*h*]quinoline-3-carboxylate, **4b**. The vibrational frequency modes were calculated by using the vibrational energy distribution analysis (VEDA) program [25]. Further, we have calculated the energy values of the highest occupied molecular orbital (HOMO) and the lowest unoccupied molecular orbital (LUMO). These energy values of HOMO–LUMO were subsequently extended to calculate electron affinity, chemical hardness, ionization potential, electronegativity, electron chemical potential, and global electrophilic index, etc. of the title molecule.

Synthesis of 2-amino-4-(4-nitrophenyl)-4H-pyrano[3,2-*h*]quinolines. A mixture of 4-nitrobenzaldehyde **1** (1 mmol), malononitrile/ethyl cyanoacetate **2** (1 mmol), 8-hydroxyquinoline **3** (1 mmol), and 30 mol.% DMAP in EtOH (5 mL) was subjected to reflux for 7 h (Scheme 1). After the complete conversion of the reactants as indicated by thin layer chromatography (TLC), the crude product was purified by column chromatography to provide the corresponding pyranoquinoline derivatives in 72–75% yield. The product was further characterized by ^{1}H NMR and IR spectral studies.

Spectral data of the compounds. 2-amino-4-(4-nitrophenyl)-4*H*-pyrano[3,2-*h*]quinoline-3-carbonitrile (**4a**): brown solid. Mp: 122–124°C. Yield: 75%. IR (KBr): ν_{max} = 3425, 3398 (NH_2), 2192 (CN) cm^{-1}. ^1H NMR (400 MHz, $CDCl_3$): δ = 5.06 (s, 1H, CH, pyran), 7.01 (s, 2H, NH_2), 7.31–8.89 (m, 9H, Ar–H). ESI-MS: m/z = = 345 (M^+ +1).

Ethyl 2-amino-4-(4-nitrophenyl)-4*H*-pyrano[3,2-*h*]quinoline-3-carboxylate (**4b**): brown solid. Mp: 162–165°C. Yield: 72%. IR (KBr): ν_{max} = 3407, 3293 (NH_2), 1681 (C=O) cm^{-1}. ^1H NMR (400 MHz, $CDCl_3$): δ = 1.28 (t, 3H, CH_3), 4.22 (q, 2H, CH_2), 5.02 (s, 1H, CH, pyran), 6.89 (s, 2H, NH_2), 7.29–8.84 (m, 9H, Ar–H). ESI-Ms: m/z = 392 (M^+ +1).

FTIR spectra were recorded in the transmittance mode using a Perkin Elmer (RX1) spectrometer in the spectral range of 4000–400 cm^{-1} with a spectral resolution of 1 cm^{-1}.

Computational method. The Gaussian 09 program was used to obtain all the computational calculations. Initially the geometry was optimized using the HF/6-311G basis set and then reoptimized using the Becke3–Lee–Yang–Parr (B3LYP) correlation function [26–28] with the 6-311G basis set. The optimized structural parameters were used for calculating vibrational frequencies, Mulliken charges, thermodynamic parameters, and several other molecular properties. HOMO–LUMO energies were determined. The vibrational frequency assignments were made accurately by using the VEDA program. Further, visual animation and verification of the normal mode of assignments was done with the Gauss View molecular visualization program [29].

Results and discussion. *Molecular geometry.* The optimized molecular structure of the ethyl 2-amino-4-(4-nitrophenyl)-4*H*-pyrano[3,2-*h*]quinoline-3-carboxylate molecule with the atomic numbering scheme is presented in Fig. 1, and the optimized geometrical parameters, namely, bond lengths and bond angles at the HF/6-311G and DFT/6-311G basis sets, are shown in Table 1. The minimum energies of the optimized structure of the title molecule calculated by the HF/6-311G and B3LYP/6-311G are –1342.41651755 and –1350.70559448 a.u. The difference in energy between these two basis sets is very small.

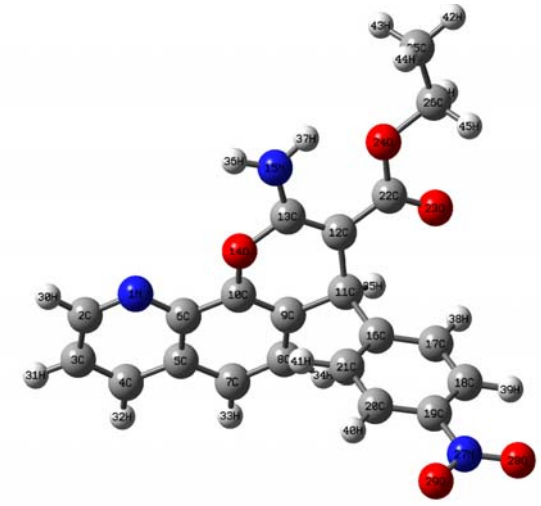

Fig. 1. Optimized structure of ethyl 2-amino-4-(4-nitrophenyl)-4*H*-pyrano [3,2-*h*]quinoline-3-carboxylate.

TABLE 1. Bond Lengths (Å) and Bond Angles (Degree) of the Title Molecule Calculated Using the HF/ 6-311G and DFT/6-311G Method

Atom No.	HF/6-311G	DFT/6-311G	Atom No.	HF/6-311G	DFT/6-311G
N1–C2	1.31	1.33	C5–C7–C8	120.35	120.36
N1–C6	1.36	1.37	C7–C8–C9	121.07	121.32
C2–C3	1.41	1.41	C8–C9–C10	118.53	118.49
C3–C31	1.06	1.08	C6–C10–C9	122.67	122.63
C4–C5	1.41	1.42	C6–C10–C14	116.66	116.35
C5–C7	1.42	1.42	C9–C10–O14	120.66	121.00
C6–C10	1.42	1.42	C9–C11–C12	110.92	110.99
C9–C10	1.35	1.37	C12–C1–N15	129.56	128.85

Continue Table 1

Atom No.	HF/6-311G	DFT/6-311G	Atom No.	HF/6-311G	DFT/6-311G
C10–O14	1.38	1.40	O14–C13–N15	109.77	109.74
C11–C12	1.52	1.53	C10–O14–C13	120.95	119.21
C13–O14	1.36	1.39	C17–C18–C19	118.83	118.88
C13–N15	1.33	1.35	C18–C19–N27	119.22	119.26
N15–H36	0.98	1.00	C12–C22–O23	124.00	125.00
N15–H37	0.98	1.00	C12–C22–O24	115.68	114.69
C16–C17	1.39	1.40	O23–C22–O24	120.31	120.29
C18–C19	1.38	1.39	N1–C2–C3	123.08	123.52
C22–O23	1.22	1.25	N1–C6–C5	122.12	122.46
C22–O24	1.36	1.41	C2–C3–C4	118.73	118.93
O24–C26	1.45	1.48	C3–C4–C5	119.68	119.78
C25–C26	1.51	1.52	C26–C25–H42	109.9	109.89
N27–O28	1.23	1.26	C20–C19–N27	119.10	119.10
N27–O28	1.23	1.26	O24–C26–H45	108.34	108.19
N27–O29	1.23	1.26	O28–N27–O29	123.14	123.34

Atomic charges. The Mulliken [30] and NBO methods were applied to calculate the total atomic charges of the title compound **4b** by using the HF/6-311G and B3LYP/6-311G basis set. Further, the approaches of Mulliken population analysis and natural bond orbital analysis were applied to obtain the atomic charge values and natural charges respectively. The charge on hydrogen atoms for the HF/6-311G method is from 0.163 to 0.431, and for the B3LYP/6-311G methods it is from 0.161 to 0.429, respectively. All hydrogen atoms and nitrogen N27 atoms show positive charge, which are acceptor atoms. The charges change with the basis set due to the polarization; for example, the charge of O14 atom is –0.553458 for HF/6-311G and –0.50748 for B3LYP/6-311G as given in Table 2. From Table 2, it can be concluded that the charges on the oxygen atom (O29, O28, O24, O23, and O14) and the nitrogen atom (N1, N15) exhibit negative values, which are donor atoms.

TABLE 2. Mulliken and NBO Charges Obtained Using the HF/6-311G and DFT/6-311G Method

Structural Parameter	HF/ 6-311G Mulliken	DFT/6-311G Mulliken	HF/6-311G NBO	DFT/6-311G NBO
N1	–0.469948	–0.322931	–0.46000	–0.42332
C2	0.090999	0.022595	0.11359	0.06207
C3	–0.269263	–0.210737	–0.24410	–0.23564
C4	–0.049372	–0.078694	–0.11654	–0.14393
C5	0.106490	0.073885	–0.08709	–0.07662
C6	–0.015519	–0.065401	0.15344	0.13645
C7	–0.139214	–0.099869	–0.16791	–0.18056
C8	–0.162779	–0.136448	–0.16168	–0.17117
C9	0.164731	0.087886	–0.05584	–0.05270
C10	0.281267	0.251209	0.33897	0.31198
C11	–0.482125	–0.516989	–0.21285	–0.24975
C12	–0.180205	–0.103944	–0.37351	–0.28300
C13	0.768311	0.692217	0.72345	0.58534
O14	–0.690907	–0.553458	–0.58183	–0.50748
N15	–0.909981	–0.837766	–0.81907	–0.75204
C16	0.179120	0.109676	0.05100	0.03010
C17	–0.230721	–0.160829	–0.20141	–0.19541
C18	–0.080621	–0.112899	–0.13113	–0.16810
C19	0.212366	0.273145	0.03274	0.06357
C20	–0.089504	–0.135336	–0.13548	–0.16994
C21	–0.136230	–0.103034	–0.21159	–0.20287
C22	0.827537	0.553204	0.91816	0.75346

Continue Table 2

Structural Parameter	HF/ 6-311G Mulliken	DFT/6-311G Mulliken	HF/6-311G NBO	DFT/6-311G NBO
O23	–0.527073	–0.428187	–0.72456	–0.63231
O24	–0.736203	–0.570868	–0.67788	–0.61282
C25	–0.516339	–0.542861	–0.53341	–0.59278
C26	–0.002155	–0.082654	0.05339	–0.02536
N27	0.168071	0.008513	0.57232	0.44151
O28	–0.386148	–0.274216	–0.44142	–0.37102
O29	–0.385872	–0.275956	–0.44324	–0.37280
H30	0.186889	0.173698	0.18127	0.19211
H31	0.182510	0.165570	0.20480	0.21356
H32	0.189931	0.168688	0.20091	0.21053
H33	0.179146	0.161874	0.20062	0.21016
H34	0.179888	0.163921	0.20476	0.21503
H35	0.228204	0.232978	0.21906	0.24213
H36	0.331452	0.350482	0.40632	0.40440
H37	0.392962	0.388198	0.43143	0.42913
H38	0.184412	0.191309	0.21943	0.23450
H39	0.233529	0.202346	0.23457	0.24100
H40	0.234238	0.200494	0.23394	0.24036
H41	0.209930	0.181514	0.20720	0.21741
H42	0.179047	0.188096	0.18692	0.20904
H43	0.178621	0.186565	0.18120	0.20052
H44	0.184454	0.187611	0.18201	0.20092
H45	0.194927	0.199330	0.16525	0.18731
H46	0.191149	0.198070	0.16380	0.18705

Vibrational analysis. The main aim of the vibrational analysis is to find vibrational modes in the compound. The titled compound ($C_{21}H_{17}N_3O_5$) with 46 atoms gives (3*N*–6) 132 vibrational modes at the B3LYP/6-311G level of theory. The vibrational assignments for these 132 vibrational levels were made using the VEDA software. DFT is an efficient and versatile method applicable to a wide variety of molecules for accurate calculations of the vibrational frequency. The calculated vibrational frequencies, IR intensities, and assignments of vibrational wave numbers along with the total energy distribution are presented in Table 3. These have been obtained by using the method B3LYP/6-311G. Most importantly, the IR absorption peak for the carbonyl group (C=O) in ethyl 2-amino-4-(4-nitrophenyl)-4*H*-pyrano[3,2-*h*]quinoline-3-carboxylate was experimentally observed at 1681 cm^{-1}.

The *ab initio* harmonic vibrational frequencies are generally stronger compared to the fundamentals observed experimentally. This is believed to be due to a combination of the electron correlation effects and insufficient basis set. However, these discrepancies were removed either by computing anharmonicity effects in the theoretical treatment or by scaling down the calculated frequency values to bridge the gap between the theoretical and observed frequencies. Importantly, the vibrational frequencies in this case have been scaled by 0.963. The calculated frequency values are in close agreement with the experimental ones, as shown in Table 3.

The experimental FTIR spectrum is presented in Fig. 2 along with FTIR spectra calculated using the DFT method. The FTIR spectrum contains some characteristic bands of the stretching vibrations of the N–H, C–H, C–C, N–C, and O–C groups. In the aromatic amines, the N–H stretching frequency occurs in the region of 3300–3500 cm^{-1}. Hence the absorption band observed was at 3407 cm^{-1} experimentally and calculated at 3426 cm^{-1} with 97% contribution. The aromatic structure shows the presence of C–H stretching vibrations in the region of 2900–3150 cm^{-1}, which is a characteristic region for the identification of the C–H stretching vibrations. In this region, the band does not affect the nature of the substituent [31]. In the present work, the experimental C–H stretching vibration were observed in the range of 3112–2911 cm^{-1}, and the calculated scaled wavenumbers in the range of 3103–2906 cm^{-1} with 99–95% contribution. The C–C stretching modes of the phenyl group are expected to be in the range from 1650–1200 cm^{-1} [32]. Therefore, the strong vibrational frequency bands at 1614, 1516, and 1219 cm^{-1} are assigned to C–C stretching vibrations experimentally, which coincides well with the calculated vibrational bands at 1619, 1520, and 1210 cm^{-1}. The ex-

perimental medium intensity band at 1018 cm^{-1} is also attributed to C-C stretching and matches well with the calculated frequency value at 1023 cm^{-1}. The FTIR bands observed at 1297 and 1189 cm^{-1} are assigned to the C–N stretching vibration and corresponding calculated wavenumbers at 1294 and 1194 cm^{-1} with the contribution of 62 and 49%, respectively (Table 3).

TABLE 3. Comparison of Experimental and Calculated Scaled Frequencies (ν, cm^{-1}) Along with the Total Energy Distribution (TED %)

$\nu_{unscaled}$	ν_{scaled}	$\nu_{experiment}$	Assignments and TED (≥15%)
3568.59	3426	3407.40	νNH 97
3232.04	3103	3112.85	νCH 96
3188.79	3061	3054.90	νCH 97
3098.16	2974	2980.79	νCH 95
3027.06	2906	2911.268	νCH 99
1686.66	1619	1614.66	νCC 60
1583.54	1520	1516.69	νCC 63
1529.26	1468	1464.26	βHCH 90
1424.51	1368	1368.08	βHCN 43
1368.72	1314	1316.18	βHCC 61
1348.33	1294	1297.07	νNC 62
1327.96	1275	1271.67	βHCC 49
1301.82	1250	1250.47	βHCC 93
1260.70	1210	1219.65	νCC 60
1243.24	1194	1189.94	νNC 49
1221.29	1172	1170.83	βHCC 40
1145.30	1099	1096.62	βHCC 47
1065.47	1023	1018.21	νCC 56
1022.08	981	971.4	γHCCH 95
889.39	854	857.06	γHCCH 25
853.27	819	823.44	νOC 34
832.43	799	794.31	βHCC 88
761.77	731	729.32	γCCCO 28
721.19	692	697.94	βCCC 38
690.84	663	664.32	rOCON 79
611.33	587	592.52	βCCO 54
550.37	528	531.81	βCCC 16
524.70	504	507.72	βCNO 16
500.34	480	471.58	γHCCC 29

N o t e. ν – stretching, β – bending, γ – out-of-plane deformation, τ – torsion.

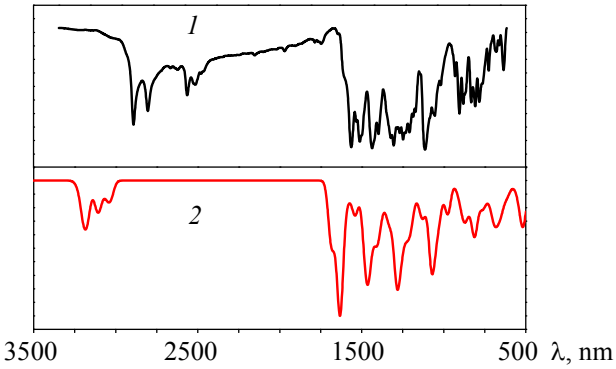

Fig. 2. Comparison of (1) experimental and (2) calculated FTIR spectra of ethyl 2-amino-4-(4-nitrophenyl)-4*H*-pyrano [3,2-*h*]quinoline-3-carboxylate.

Frontier molecular orbital analysis and related molecular properties. Frontier orbitals are the name given to the highest occupied molecular orbital (HOMO) and the lowest-lying unoccupied molecular orbital (LUMO), which are the most important orbitals in a molecule. HOMO and LUMO represent electron donating and electron accepting capability, respectively. The pictorial representation and the energy difference for the title molecule are shown in Fig. 3. The calculated energy value of HOMO is –6.24 eV, and the energy value of LUMO is –2.82 eV. The value of the energy difference between the HOMO and LUMO is 3.42 eV. Further, eventual charge transfer interactions within the molecule are clearly indicated by the frontier orbital gap [33]. It is important to mention that the energy gap and subsequent electronic transition between HOMO–LUMO is lowest in a molecule, and this energy gap helps us to recognize the molecule kinetic stability and chemical reactivity [34, 35]. The HOMO energy, LUMO energy, energy difference (ΔE), electron affinity (A), chemical potential (μ), ionization potential (I), global electrophilicity (ω), and global hardness (η) for the title molecule have been calculated at the level B3LYP/6-311G, and the results are summarized in Table 4.

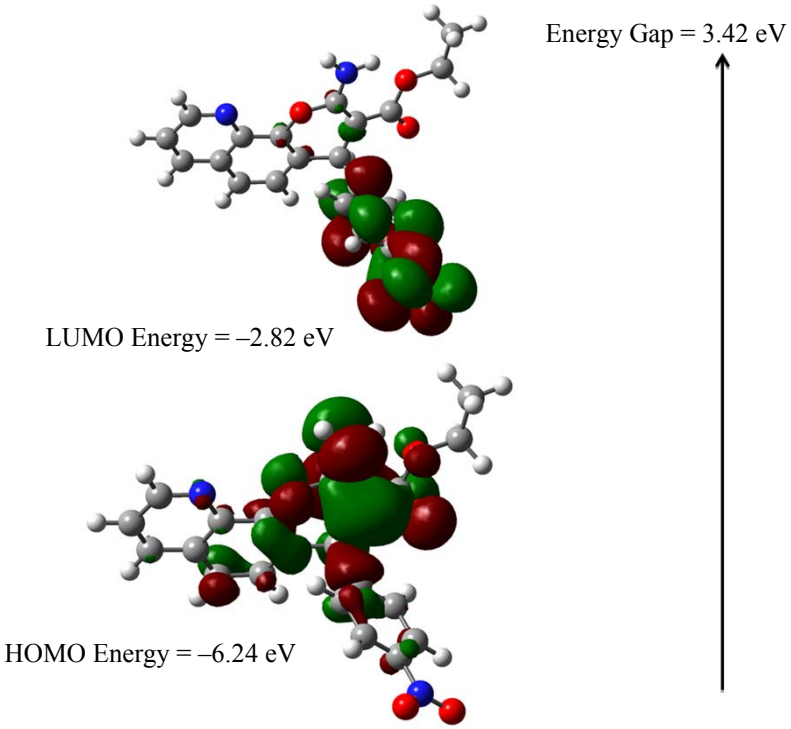

Fig. 3. Pictorial representation of molecular orbitals of ethyl 2-amino-4-(4-nitrophenyl)-4*H*-pyrano[3,2-*h*]quinoline-3-carboxylate.

TABLE 4. HOMO, LUMO, and Other Related Molecular Parameters

Molecular Parameters (eV)	DFT/6-311G
E_{HOMO}	–6.24
E_{LUMO}	–2.82
$\Delta E = E_{LUMO} – E_{HOMO}$ energy	3.42
Ionization Potential (I)	6.24
Electron Affinity (A)	2.82
Global Hardness (η)	1.71
Chemical Potential (μ)	4.53
Global Electrophilicity (ω)	6.0

TABLE 5. Thermodynamic Properties at Different Temperatures at the DFT/6-311G Level

Thermodynamic Parameters (298.15 K)	B3LYP/6-311G
SCF energy	–1350.70559448
Total energy (Thermal), E_{total} (kcal/mol)	236.190
Vibrational energy, E_{vib} (kcal/mol)	234.412
Zero point vibrational energy, E_0 (kcal/mol)	221.10474
Heat Capacity, C_v (cal · mol^{-1} · K^{-1})	93.022
Entropy, S (cal · mol^{-1} · K^{-1})	170.963
Rotational Constants (GHz)	
A	0.17434
B	0.12069
C	0.08143
Dipole moment (Debye)	
μ_x	6.6462
μ_y	4.5867
μ_z	0.7581
μ_{total}	8.1108

TABLE 6. Thermodynamic Properties of the Ethyl 2-Amino-4-(4-Nitrophenyl)-4*H*-Pyrano [3,2-*h*] Quinoline-3-Carboxylate Molecule at Different Temperatures.

Temperature	Heat Capacity (cal · mol^{-1} · K^{-1})	Entropy (cal · mol^{-1} · K^{-1})	Total thermal energy (kcal/mol)
50	23.913	81.455	221.861
100	37.415	103.659	223.392
150	50.585	122.105	225.589
200	64.491	139.116	228.463
250	78.977	155.499	232.048
300	93.557	171.552	236.362
350	107.695	187.351	241.396
400	120.976	202.875	247.117
450	133.166	218.073	253.476
500	144.190	232.894	260.414
550	154.081	247.298	267.876
600	162.930	261.265	275.805
650	170.850	274.784	284.153
700	177.955	287.857	292.877

Thermodynamic properties. The thermodynamic parameters such as thermal energy, heat capacity, entropy, rotational constants, dipole moment, etc. were calculated using the HF and DFT method at 298.15 K in the ground state and are presented in Table 5. Subsequently, the statistically thermodynamic parameters such as heat capacity (C), entropy (S), and enthalpy (H) for the title molecule were calculated using B3LYP/6-311G at various temperatures ranging from 50 to 700 K, and the results are summarized in Table 6. From the correlation graph of heat capacity, entropy, and enthalpy (Fig. 4), it is observed that these parameters increase with increase in temperature. This is due to the fact that with increasing temperature the molecular vibrational intensity increases [36], and hence these parameters increase as they are directly related to the vibrational intensity. Quadratic formulas were used to fit the correlation equations between different parameters such as enthalpy, heat capacity, entropy, and temperature, R being the corresponding fitting factor (R^2) for these thermodynamic parameters, and the resultant fitting equations are as presented below:

$$H_m = 220.47946 + 0.0162T + 1.25822\times10^{-4}T^2,\ R^2 = 0.99981,$$

$$C_{p,m} = 5.44398 + 0.33342T - 1.19779\times10^{-4}T^2,\ R^2 = 0.99971,$$

$$S_m = 64.20158 + 0.38829T - 9.9639\times10^{-5}T^2,\ R^2 = 0.99973.$$

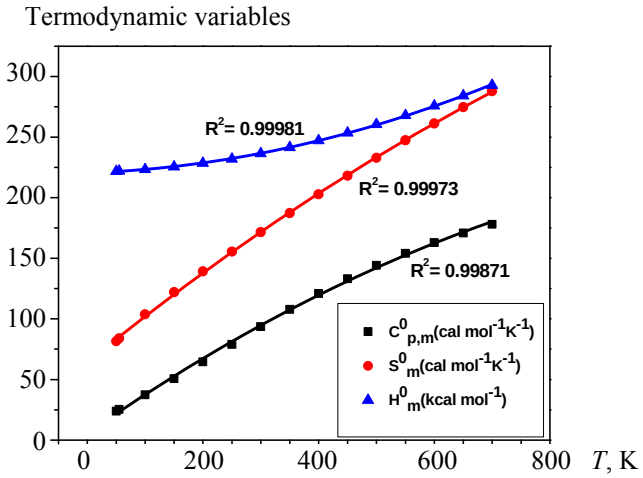

Fig. 4. Correlation graph between the thermodynamic properties and temperature.

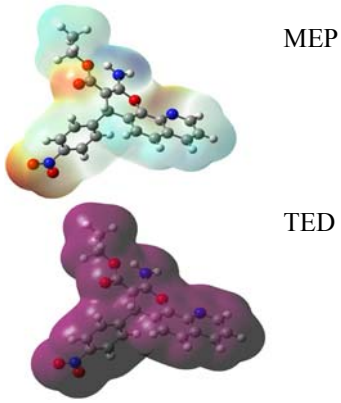

Fig. 5. Total electron density and molecular electrostatic potential maps of ethyl 2-amino-4-(4-nitrophenyl)-4*H*-pyrano [3,2-*h*]quinoline-3-carboxylate.

Total electron density (TED) and molecular electrostatic potential (MEP) maps are constructed using the DFT theory with the 6-311G level, and 3D plots of these are shown in Fig. 5. The ED plot shows a uniform distribution for the title compound. MEP is related to the electron density isosurface, which depicts the charge density, delocalization, site of chemical reactivity, and size and shape of the molecules. These results may be used to predict the site on the molecule for a probable electrophilic attack. The molecular electrostatic potential surface is a plot of ESP mapped onto the constant ED surface. This represents molecular size and electrostatic potential in terms of color coding. MEP mapping is useful in the study of molecular structure with its physiochemical property relationships [37–39]. Further, MEP is effectively applied for the qualitative analysis of nucleophilic and electrophilic reactions for further study of biological processes and hydrogen bonding interactions [40]. The MEP surface is a useful property and gives essential information about the reactive sites. As can be seen from the MEP plot, the surface over all the hydrogen atoms (H) shows maximum positive potential (site for nucleophilic attack) and the surface over the oxygen and nitrogen atoms shows the site for electrophilic attack.

Conclusion. An efficient route to pyranoquinolines is established *via* three component reaction of 4-nitrobenzaldehyde, malononitrile/ethyl cyanoacetate, and 8-hydroxyquinoline. The optimized molecular structure, atomic charges, and vibrational frequencies have been calculated by the DFT/B3LYP method with the 6-311G basis set. The HOMO–LUMO energies and frontier orbital energy gap show that the energy transfer occurs within the molecule. The correlations between the thermodynamic parameters and temperature were also obtained and show that an increase in temperature causes an increase in heat capacities, entropies, and enthalpies. The molecular orbitals and MESP surfaces are also plotted.

REFERENCES

1. S. M. Wickel, C. A. Citron, J. S. Dickschat, *Eur. J. Org. Chem*., 2906−2913 (2013).
2. J. A. Makawana, M. P. Patel, R. G. Patel, *Arch. Pharm*., **345**, 314−322 (2012).
3. Y. Deng, J. P. Lee, M. Tianasoa-Ramamonjy, J. K. Synder, S. A. D. Etages, D. Synder, M. P. Kanada, C. J. Turner, *J. Nat. Prod*., **63**, 1082–1089 (2000).
4. N. A. Keiko, L. G. Stepanova, M. G. Voronkov, G. I. Potapova, N. O. Gudratov, E. M. Treshchalina, *J. Pharm. Chem*., **36**, 407–409 (2002).
5. S. Prado, H. Ledeit, S. Michel, M. Koch, J. C. Darbord, S. T. Cole, F. Tillequin, P. Brodin, *Bioorg. Med. Chem*., **14**, 5423–5428 (2006).
6. A. R. Saundane, K. Vijaykumar, A. V. Vaijinath, *Bioorg. Med. Chem. Lett*., **23**, 1978−1984 (2013).
7. P. G. Pietta, *J. Nat. Prod*., **63**, 1035–1042 (2000).
8. M. D. Aytemir, B. Özçelik, *Eur. J. Med. Chem*., **45**, 4089–4095 (2010).
9. P. W. Smith, S. L. Sollis, P. D. Howes, P. C. Cherry, I. D. Starkey, K. N. Cobley, H. Weston, J. Scicinski, A. Merritt, A. Whittington, P. Wyatt, N. Taylor, D. Green, R. Bethell, S. Madar, R. J. Fenton, P. J. Morley, T. Pateman, A. Beresford, *J. Med. Chem*., **41**, 787–797 (1998).
10. A. Venkatesham, R. S. Rao, K. Nagaiah, J. S. Yadav, G. RoopaJones, S. J. Basha, B. Sridhar, A. Addlagatta, *Med. Chem. Commun*., **3**, 652−658 (2012**)**.
11. L. Bonsignore, G. Loy, D. Secci, A. Calignano, *Eur. J. Med. Chem.*, **28**, 517–520 (1993).
12. D. Armetso, W. M. Horspool, N. Martin, A. Ramos, C. Seoane, *J. Org. Chem*., **54**, 3069–3072 (1989).
13. K. H. Lee, S. M. Kim, J. Y. Kim, Y. K. Kim, S. S. Yoon, *Bull. Korean Chem. Soc*., **31**, 2884–2888 (2010).
14. R. Klingenstein, P. Melnyk, S. R. Leliveld, A. Ryckebusch, C. Korth, *J. Med. Chem*., **49**, 5300–5308 (2006).
15. S. Vandekerckhove, H. G. Tran, T. Desmet, M. D'hooghe, *Bioorg. Med. Chem. Lett*., **23**, 4641–4643 (2013).
16. K. C. Fang, Y. L. Chen, J. Y. Sheu, T. C. Wang, C. C. Tzeng, *J. Med. Chem*., **43**, 3809–3812 (2000).
17. A. K. Sadana, Y. Mirza, K. R. Aneja, O. Prakash, *Eur. J. Med. Chem*., **38**, 533–536 (2003).
18. Y. L. Chen, I. L. Chen, C. M. Lu, C. C. Tzeng, L. T. Tsao, J. P. Wang, *Bioorg. Med. Chem*., **12**, 387–392 (2004).
19. G. Barbosa-Lima, A. M. Moraes, A. S. Araújo, E. T. Silva, C. S. Freitas, Y. R. Vieira, A. Marttorelli, J. C. Neto, P. T. Bozza, M. V. N. Souza, T. M. L. Souza, *Eur. J. Med. Chem*., **127**, 334–340 (2017).
20. K. Rurack, A. Danel, K. Rotkiewicz, D. Grabka, M. Spieles, W. Rettig, *Org. Lett*., **4**, 4647–4650 (2002).
21. F. Liang, Z. Xie, L. Wang, X. Jing, F. Wang, *Tetrahedron Lett*., **43**, 3427–3430 (2002).
22. N. J. Parmar, R. A. Patel, B. D. Parmar, N. P. Talpada, *Bioorg. Med. Chem. Lett*., **23**, 1656 (2013).
23. P. Gunasekaran, P. Prasanna, S. Perumal, *Tetrahedron Lett*., **55**, 329 (2014).
24. *Gaussian 09, Revision A.1*, Gaussian, Inc., Wallingford, CT (2013).
25. M. H. Jamroz, *Vibrational Energy Distribution Analysis VEDA* 4, Warsaw (2004).
26. A. D. Becke, *J. Chem. Phys*., **98**, 5648 (1993).
27. A. D. Becke, *Phys. Rev. A*, **38**, 3098 (1988).
28. C. Lee, W. Yang, R. G. Parr, *Phys. Rev. B*, **37**, 785 (1988).
29. A. Frisch, A. B. Neilson, A. J. Holder, *GAUSSVIEW User Manual*, Gaussian Inc. Pittsburgh, PA (2000).
30. R. S. Mulliken, *J. Chem. Phys*., **23**, 1833 (1955).
31. H. Tanak, Y. Köysal, Y. Ünver, M. Yavuz, S. Isık, K. Sancak, *Mol. Phys*., **108**, 127 (2010).
32. S. Muthu, E. I. Paulraj, *Solid State Sci*., **14**, 476 (2012).
33. R. Mathammal, N. Jayamani, N. Geetha, *J. Spectrosc*., **2013**, 171735 (2013).
34. E. Kavitha, N. Sundaraganesan, S. Sebastian, *Ind. J. Pure Appl. Phys*., **48**, 20–30 (2010)
35. A. Jayaprakash, V. Arjunan, S. Mohan, *Spectrochim. Acta, A*, **81**, 620–630 (2011).
36. J. BevanOtt, J. Boerio-Goates, *Chemical Thermodynamics: Principles and Applications*, Academic Press, San Diego (2000).
37. I. Fleming, *Frontier Orbitals and Organic Chemical Reactions*, John Wiley and Sons, New York (1976).
38. J. M. Semanario, *Recent Developments and Applications of Modern Density Functional Theory*, **4**, Elsevier, The Netherlands (1996).
39. T. Yesilkaynak, G. Binzer, F. Mehmet Emen, U. Florke, N. Kulcu, H. Arslan, *Eur. J. Chem*., **1**, 1 (2010).
40. B. Kosar, C. Albayrak, *Spectrochim. Acta, A*, **78**, 96 (2011).